Journal of Nuclear Materials 173 (1990) 214–228
North-Holland

MISTRAL: A COMPREHENSIVE MODEL FOR TRITIUM TRANSPORT IN LITHIUM-BASE CERAMICS
Part II: Comparison of model predictions with experimental results *

G. FEDERICI, A.R. RAFFRAY and M.A. ABDOU

Mechanical, Aerospace and Nuclear Engineering Department, University of California at Los Angeles, Los Angeles, CA 90024-1597, USA

Received 20 November 1989; accepted 1 May 1990

A new tritium transport model called MISTRAL (Model for Investigative Studies of Tritium Release in Lithium Ceramics) has been developed to describe and predict the kinetics of tritium release in lithium ceramic materials for tritium breeding applications in fusion blankets. The model has transient capabilities and has been developed to analyze the full range of transient conditions produced in in-pile tritium recovery experiments and expected in fusion blankets. Calibration of the model against experiments has been done in parallel with its development in order to assess its predictive capabilities and to identify the ranges of potential applicability. The comparisons of the results available for lithium metasilicate and aluminate samples irradiated respectively in the two in-pile tritium recovery experiments LISA1 and MOZART are presented and discussed in this paper. They have been selected for the calibration of the codes as being good examples of various features relevant for tritium release analysis in ceramic breeders under different transient conditions such as change in temperature, purge gas composition and reactor power.

1. Introduction

In recent years, considerable progress has been made in identifying tritium transport and release mechanisms in tritium breeding ceramics for fusion blankets and in gaining a better understanding of the synergistic interplay of the several processes which seem to take place and affect the overall tritium release kinetics. This understanding has evolved through both experimental and theoretical work and is aimed at the development of predictive capabilities which are necessary and highly desirable to design, construct and operate effectively solid breeder components.

Furthermore, completed and on-going in-pile tritium recovery experiments have better identified potentially important variables which can strongly affect the tritium inventory and the kinetics of the release. Indeed, factors such as solid breeder microstructure (i.e. specific surface area, grain size and pore size distribution) and chemical composition, activation energies for bulk diffusion and for adsorption and desorption phenomena, and purge gas composition have been found to play crucial roles in determining the fractions of tritium released and retained in ceramic materials.

Therefore, in the current phase of research and development, there is a strong incentive to develop more sophisticated predictive capabilities which are necessary to understand the new experimental data available and to extrapolate them to different ranges of conditions of interest.

As yet, no single fundamental method of calculating tritium release exists, the major reasons being: (1) many potentially important variables are involved, the mathematical description of which may be complex, (2) the data against which the hypothesis can be tested are themselves subject to considerable uncertainties; (3) sometimes empirical release terms based, for example, on apparent diffusion or desorption coefficients, have been correlated reasonably well with existing data, making the development of a rigorous fundamental model less attractive. However, to better understand the observed results that are becoming available from the experiments and to extrapolate them to different ranges of interest, as well as to plan and design experiments in order to maximize their benefits, there is a strong need to develop more comprehensive models.

* Work supported by the US Department of Energy under grant #DE-FG03-86ER52123

In particular, it is important for the model to properly describe the underlying physics, since fits with physically unsound models to experimental data by adopting suitable parameters may fail whenever extrapolations are needed to new ranges of operating conditions. In the early models tritium release from ceramic materials was interpreted as bulk diffusion controlled and only recently an attempt has been made by Kopasz et al. [1] to include a simplified desorption flux boundary condition. In general, however, these models were unable to satisfactorily describe and interpret many of the experimental data available and to fully characterize the influence of several key factors on the kinetics of tritium release.

We have proposed and developed a comprehensive model for tritium transport in fine-grained solid breeder media [2–4]. It includes as steps of the transport sequence leading to release: tritium diffusion through the grain and along the grain boundaries; adsorption and desorption at the breeder surface; and diffusion through the network of pores. A key improvement of the model covers a better phenomenological and theoretical characterization of the processes at the solid/gas interface and their crucial linking to the bulk and pore regions. A thorough description of the model MISTRAL including analytical and numerical formulations, together with its computational capability and the ranges of potential applicability are reported in Part I of this paper [5]. The model has been applied over a wide range of transient operating conditions and can be regarded as a state-of-the-art model based on the current level of understanding of tritium transport and release behavior in lithium-base solid breeder materials.

To validate the results provided by this model and to assess its predictive capability, it is necessary to compare its results with reliable experimental results. Two recent and well characterized in situ tritium extraction experiments from lithium base breeder materials, LISA1 [6] and MOZART [7], have been selected for the model and code validation. They provide good examples of tritium behavior in ceramic breeder materials under different transient operating conditions, such as changes in temperature, changes in purge gas composition and changes in reactor power.

The features of the experiments selected for the code calibration along with the data and material properties used for the analysis are described in the next section. Section 4 presents the results of the calculation and the comparison of model predictions for tritium release with experimental data. This is followed by a summary section. The symbols and notations are given in a separate nomenclature section.

2. Calibration of the model against experiments

In order to generate confidence in the results provided by the model MISTRAL and to assess its predictive capability, it is necessary to compare its results with reliable experimental data. The proposed calibration analysis is aimed at defining the confidence level of the predictions for the ranges of parameters and the operating conditions to which the code can be applied and to assess the influence of key variables affecting the overall kinetics of tritium release. The calibration analysis of the model MISTRAL has represented in this concern a very important phase and has been carried out in parallel with its development.

2.1. Selection of benchmarks

Two recent in situ tritium extraction experiments, LISA1 and MOZART, have been selected as benchmarks for the analysis since they provide good examples of tritium release behavior in ceramics breeders under transient operating conditions. Table 1 summarizes the experiments and the breeder materials considered for this proposed analysis. In particular, the MOZART experiment has been described thoroughly in reports and represents the most complete set of information including material properties data and reactor performance history, and, thus, provides a good benchmark for testing the adequacy and accuracy of a model. The LISA1 experiment which was conducted at the SILOE reactor in Grenoble (France) had six breeder capsules, four with Li_2SiO_3, one with Li_4SiO_4 and one with $LiAlO_2$. Each capsule was separately purged. Irradiation began on October 25, 1985, and was continued for three-week cycles. The testing included systematic variation of four parameters: temperature (450 to 730 °C), neutron flux (0.8 to 2.7×10^{17} m^{-2} s^{-1}), sweep gas flow

Table 1
Experiments considered for the analysis

Experiment	Material	Year	Remarks (main parametric effects)
LISA1			
Sample P1	Li_2SiO_3	1985	Effect of a temperature change on the tritium release
MOZART			
Sample S1	$LiAlO_2$	1988	Effect of a temperature change and purge gas composition change (addition of H_2) on the tritium release

Table 2
Investigated LISA1 test matrix for sample P1, Li_2SiO_3 (reference values [6]; tritium generation rate, $\mathscr{G}^* = 8.5\times10^{18}$ atoms/m^3 s); purge flow rate, $\Gamma^* = 2.5$ l/h; temperature, $T^* = 650\,^\circ$C)

Cycle and run	Date started	Sweep gas	$\mathscr{G}/\mathscr{G}^*$	Γ/Γ^*	T
A-1	25 Oct. 85	He	$0 \Rightarrow 1$	1	T^*
A-2	28 Oct. 85	He	1	1	$T^* \Rightarrow T^* - 50$
A-3	29 Oct. 85	He	1	1	$T^* - 50 \Rightarrow T^*$
A-4	30 Oct. 85	He	1	1	$T^* \Rightarrow T^* - 50$
A-5	2 Nov. 85	He	1	1	$T^* - 50 \Rightarrow T^* - 100$

Table 3
Investigated MOZART test matrix for sample S1, $LiAlO_2$ (reference values [8]: tritium generation rate, $\mathscr{G}^* = 5.47\times10^{18}$ atoms/m^3 s; purge flow rate, $\Gamma^* = 2.4437$ l/h; temperature, $T^* = 650\,^\circ$C)

Run	Date started	Sweep gas	$\mathscr{G}/\mathscr{G}^*$	Γ/Γ^*	T
2.7	26 March 88	He + 0.1% H_2 ⇒ He	1	1	T^*
3.4	14 April 88	He ⇒ He + 0.01% H_2	1	1	T^*
3.5	22 April 88	He + 0.01% H_2	1	1	$T^* \Rightarrow T^* - 50$
3.6	24 April 88	He + 0.01% H_2	1	1	$T^* - 50 \Rightarrow T^*$
4.4	8 May 88	He + 0.01% H_2 ⇒ ...	$1 \Rightarrow 0.85$	1	$T^* - 100$
		... ⇒ He + 0.1% H_2	$0.85 \Rightarrow 1$		

Table 4
Properties data and parameters used for the analysis

	Experiment	
	LISA1	MOZART
Sample	P1	S1
Material	Li_2SiO_3	$LiAlO_2$
Tritium generation rate, $\mathscr{G}$ (atoms/m^3 s)	8.5×10^{18}	5.47×10^{18}
Grain radius, r_g (10^{-6} m)	35	≈1
Specimen dimensions, (10^{-3} m)	$7.2(\phi)\times42.6$	$8(\phi)\times30$
Density (TD), ρ (kg/m^3)	2530	2610
Porosity, ϵ_p (open porosity)	0.135 (0.123)	0.19 (0.19 assumed)
Tortuosity, δ	$1/\epsilon_p$	$1/\epsilon_p$
Pore diffusion factor, f_{DP}	0.02	0.04
BET area, S_{BET} (m^2/Kg)	1000 (parameter)	770
Purge flow composition	pure He	He + % H_2
Purge flow rate, Γ (l/h)	2.5	2.44
Grain diffusion pre-exponential, D_{g0} (m^2/s)	7.9×10^{-10} [19]	1.99×10^{-9} [19]
Grain diffusion activation energy, E_g (kJ/mol)	77.4 [19]	90.4 [19]
Bulk adsorption pre-exponential, β_0 (m/s)	$1\times10^{13}/\sqrt{N_s}$ [20]	$1\times10^{13}/\sqrt{N_s}$ [20]
Bulk adsorption activation energy, E_β (kJ/mol)	10 (parameter)	10 (parameter)
Adsorption activation energy, E_{ads} (kJ/mol)	20	20
Heat of adsorption as a function of θ, $Q(\theta)$ (kJ/mol)	(Fischer's data) [10] (at about 600 °C)	(Fischer's data) [10] (at about 600 °C)
Desorption activation energy, $E_{des}(\theta)$ (kJ/mol)	$E_{ads} + Q(\theta)$	$E_{ads} + Q(\theta)$

rate (1.8 to 7.0 l/h), and sweep gas composition (He, He + 0.1% H_2, He + 0.2% O_2). For the calibration analysis, sample P1 (lithium metasilicate) was selected and the results of the model are presented and discussed for temperature transients for a pure helium purge stream with no hydrogen in the system.

The MOZART experiment [8,9] was carried out within the framework of the BEATRIX program, as a part of the Commissariat à l'Energie Atomique (CEA) contribution to this international collaboration program. The experiment was conducted for 45 days in the Melusine reactor at Grenoble (France). Ceramics investigated were Li_2O and $LiAlO_2$ from the Japan Atomic Energy Research Institute (JAERI) and CEA and Li_2ZrO_3 from Argonne National Laboratory (ANL). Hence, the name of MOZART (Melusine Oxide Zirconate Aluminate Release of Tritium) which was given to the experiment. The experimental results showed the favorable effect of hydrogen addition to the purge gas on the tritium release, which is an indication of the dominant contribution of surface processes on the tritium release response. The influence of parameters such as temperature and sweep gas composition was thoroughly investigated in this experiment. Sample S1 (lithium aluminate) was selected as example for the calibration analysis, and the model predictions are presented and discussed in this paper for temperature transients and particularly for purge gas composition transients.

2.2. Data and material properties for the analysis

Tables 2 and 3 show for the LISA1 and MOZART experiments, respectively, the details of the test matrix for the selected samples which have been investigated. The property data and parameters used in the analysis are summarized in table 4.

In theoretical models of tritium release from ceramic breeders, the activation energy of desorption, $E_{des}(T, \theta)$, as a function of the coverage and of the temperature, is an important variable. Estimates of this quality may be made from the heat of adsorption, $Q(T, \theta)$, on the basis that the activation energy of desorption is equal to the sum of the heat of adsorption and the activation energy of adsorption (i.e., $E_{des}(T, \theta) = E_{ads}(T, \theta) + Q(T, \theta)$). Usually, the activation energy of adsorption is small, and the activation energy of desorption tends to vary with coverage in the same way as the heat of adsorption does. Data have been recently obtained by Fischer [10] on surface adsorption of $H_2O_{(g)}$ in $LiAlO_2$ at temperatures up to 873 K and under a helium purge gas containing small quantities of H_2O. Adsorption of $H_2O_{(g)}$ on the BET surface for fusion reactor blanket situations is complicated by the use of H_2 in the helium purge to enhance tritium release. Coadsorption of the two gases must be considered. In this connection, it is interesting that the adsorption of H_2 on alumina reported by Gruber [11] shows, like the result obtained by Fischer for $LiAlO_2$–$H_2O_{(g)}$, a minimum in adsorption at about 573 K. However, the degree of adsorption is likely to be lower for H_2 than for H_2O because, even for the relatively high H_2 partial pressures of 0.25 atm (2.5×10^4 Pa), the adsorption amounted to only about $\theta = 0.001$. Measurements of adsorption under such conditions are needed. Note that, even though the data available are for the $LiAlO_2/H_2O$ system, it is believed that desorption of H_2 only occurs as H_2O and thus the desorption activation energies for both H_2 and H_2O are likely to be similar. Because Fischer's data are at present the only set of data available for any lithium-base ceramic materials, they have been used as reference for the calculation.

The modeling of the experimental results has been carried out according to the following strategy:

- represent the experimental conditions for each sample (i.e., temperature history, purge flow and purge gas composition histories, as well as tritium generation rate history) as closely as possible;
- use for the analysis all available physical and chemical properties for the breeder of interest.

In the light of the above and because most of the experimental database and key material properties crucial for tritium modeling studies in solid breeder ceramics, such as specific surface area, porosity, adsorption and desorption surface properties, are currently available only for lithium aluminate, the analysis has mostly focussed on $LiAlO_2$ samples.

Of particular significance is the attempt to minimize the number of parameters (i.e. controlling knobs) that can be varied to match the model to the experimental results, and to use measured physical and chemical properties when available, which both provide the best test for the adequacy and accuracy of the model. For the given set of input data, the only important process that can be controlled is pore diffusion through selection of the tortuosity and pore diffusion factors [5], which is discussed in the next section.

2.3. Pore diffusion

Diffusion through the pores is strongly affected by the ceramic breeder porosity characteristics, in particular by the amount of open porosity and by the magni-

tude and distribution of pore sizes. The effective diffusive path length is dependent on the open porosity which is actually used in the model of Wakao et al. [12] to determine the tortuosity factor ($\delta = 1/\epsilon_p$). The local diffusion regime (Knudsen, ordinary or transition) in the pore depends on the local pore size, and the averaging of the local diffusion coefficient over the distribution of pore sizes can result in an average diffusion coefficient quite different from that obtained from the average pore radius. In addition, a series of constrictions and expansions as dictated by the pore size distribution can significantly lower the effective pore diffusion coefficient.

The tortuosity factor is used to account for the diffusive path length being longer than the physical dimension of the porous material. It is dependent on the amount of open interconnected porosity and would be affected by pore closure due to temperature and/or irradiation sintering. Here, the tortuosity factor is estimated from the model of Wakao et al. [12]. However, one has to keep in mind that tortuosity factors can cover a wide range of values depending on the material form and microstructure and can be much higher than the value obtained from the above model, as indicated by the experimental data of Krasuk et al. [13], for example.

Data on pore size distribution for lithium ceramics are scarce, a notable exception being the silicates, including those used in the LISA1 experiment, whose porosity distributions are characterized in ref. [14]. Fig. 1 shows the pore size distribution in terms of the open porosity associated with each mean pore diameter for the LISA1 Li_2SiO_3 sample considered here, based on the data from ref. [14]. The distribution covers a wide range of pore sizes and can be considered bimodal with distribution peaks corresponding to mean pore diameters of about 35 and 1500 nm.

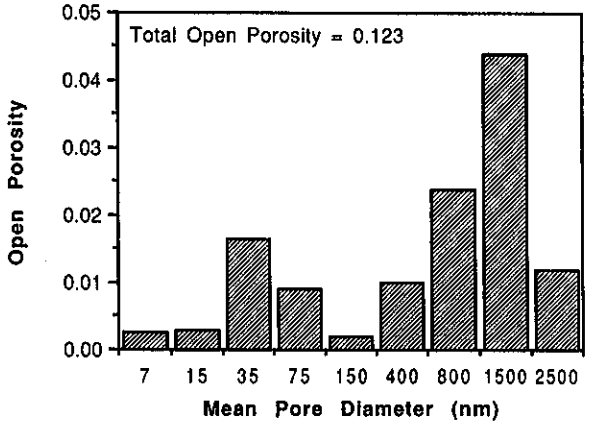

Fig. 1. Open porosity associated with different mean pore diameters for the LISA1 Li_2SiO_3 sample (from ref. [14]).

The series of expansions and constrictions associated with different pore sizes can significantly affect the effective pore diffusion. For example, Michaels [15] considered two cylindrical pores, one of radius r_{p1} and length l_{p1} and the other of radius r_{p2} and length l_{p2}, which are connected in series. The pore system may be considered as composed of any number of these characteristic units in series. Since the diffusional resistance offered by any one of these units is the same as any other, it is possible by characterizing the unit to characterize thereby the entire pore. By assuming the same flux through each cylindrical pore and through an equivalent uniform pore of average volume per unit length similar to that of the unit, Michaels derived the following equation:

$$\frac{D_{p_{ave}}}{D_{p_{eff}}} = 1 + \frac{L_p}{(L_p+1)^2}\left(\frac{R_p^2-1}{R_p}\right)^2, \quad (1)$$

where $D_{p_{ave}}$ is the average pore diffusion coefficient through each cylindrical pore, $D_{p_{eff}}$ is the effective pore diffusion coefficient due to constriction and expansion effects, $L_p = l_{p_1}/l_{p_2}$, and $R_p = r_{p_1}/r_{p_2}$.

In the absence of specific microscopic information about pore geometry, a reasonable assumption is that the length of a bulge or constriction is proportional to its diameter (i.e., $L_p = R_p$). In that case for the LISA1 Li_2SiO_3 sample ($R_p = 1500/35 = 43$):

$$D_{p_{eff}}/D_{p_{ave}} = 0.023. \quad (2)$$

It is important to note that the above reduction in the pore diffusion coefficient is solely due to a series of constrictions and expansions in the pore diffusive path and was obtained using a constant $D_{p_{ave}}$ independent of the pore size. This is the case if ordinary diffusion prevails. However, if diffusion occurs even partially in the Knudsen or transition regimes, $D_{p_{ave}}$ should then be estimated as an average pore diffusion coefficient by taking into account the pore size distribution. The value of this average pore diffusion coefficient based on the pore size distribution can be quite different from the value obtained from the average pore radius. For the Li_2SiO_3 sample, for example, the average radius of the pore system (assumed interconnected), r_{ip}, is 0.124 μm and the corresponding diffusion coefficient, D_p, is 1.26 $\times 10^{-4}$ m^2/s for diffusion in the transition regime.

From fig. 1, the local porosity, ϵ_{p_j}, and the associated pore radius, r_{p_j}, can be combined to obtain an

effective characteristic length, $(\epsilon_{p_j}/r_{p_j}^2)$, for diffusion through each pore size, j. The diffusion coefficient, D_{p_j}, associated with each pore size can be calculated based on the local diffusion regime. The time constant for diffusion through each pore size is then given by $(\epsilon_{p_j}/r_{p_j}^2 D_{p_j})$. The average diffusion coefficient, $D_{p_{ave}}$, can then be estimated by equating the summation of time constants for diffusion through each pore size to the overall time constant for diffusion.

$$D_{p_{ave}} = \frac{\left(\Sigma_{j=1}^{n}\left(\epsilon_{p_j}/r_{p_j}^2\right)\right)^2}{\Sigma_{j=1}^{n}\left(\epsilon_{p_j}/r_{p_j}^2 D_{p_j}\right)}. \quad (3)$$

Doing this calculation for the LISA1 Li_2SiO_3 sample yields:

$$D_{p_{ave}}/D_p = 0.14. \quad (4)$$

Thus, combining the effects of changes in the local pore diffusion coefficient with those of constrictions and expansions in the interconnected pore system (eqs. (2) and (4)) results in:

$$D_{p_{eff}}/D_p = 0.0033. \quad (5)$$

This value gives a good indication of what the effective pore diffusion coefficient should be but still carries some uncertainty. For example, the effect of constrictions and expansions was estimated assuming only two pore sizes for calculation simplicity. Accounting for the numerous pore sizes shown in fig. 1 might yield a different answer. For this reason, it was decided to set f_{DP} to a high value of 0.02 to obtain the reference value of the pore effective diffusion coefficient, $D_{p_{eff}}$(ref.), for the Li_2SiO_3 sample. This reference value was then changed by factors of 0.1 and 0.01 to cover a possible range of uncertainty and to assess the effect of the pore diffusion coefficient on the tritium release.

For the $LiAlO_2$ sample from MOZART, the situation is not as clear since detailed data on the pore size distribution are unavailable. If the pore size distribution is as wide as that of the Li_2SiO_3 sample, then $D_{p_{eff}}$ might be lower than D_p by a factor of the order of 300. It is also possible that the pore size distribution is not bimodal. In view of these uncertainties, it seemed prudent to set a moderate value of f_{DP} in order to obtain the reference value of the effective pore diffusion coefficient, which could then be varied as a parameter in order to reproduce the experimental tritium release characteristics. Based on this, a value of $f_{DP} = 0.04$ was chosen for calculating $D_{p_{eff}}$(ref.) for the $LiAlO_2$ sample.

Note that because of the combined effect of the effective pore diffusion coefficient and of the interconnected pore path length on the calculation of the tritium release, varying $D_{p_{eff}}$(ref.) for a parametric analysis in effect covers uncertainties both in the effective pore diffusion coefficient and in the tortuosity.

Results of the transient analyses carried out using the model MISTRAL are presented and discussed in the next section.

3. Comparison of model predictions for transient release with experimental results

3.1. Transient tritium recovery behavior after a temperature change

As indicated by the authors previously [3], modeling studies on the behavior of tritium transport during temperature transient conditions in a lithium metasilicate sample irradiated in the LISA1 experiments resulted in the identification of important factors affecting the release response, such as the ceramic breeder microstructure (e.g., grain size, breeder specific surface area, pore characteristics) and the desorption activation energy. Here, results of the analysis carried out for the Li_2SiO_3 (metasilicate) sample P1 irradiated in the LISA1 experiment and for the $LiAlO_2$ sample S1 irradiated in the MOZART experiment are presented and discussed.

3.1.1. Results of the analysis

For the case of a metasilicate, figs. 2 and 3 show the effect of a change in the pore diffusion coefficient on the tritium release kinetics and the surface coverage for

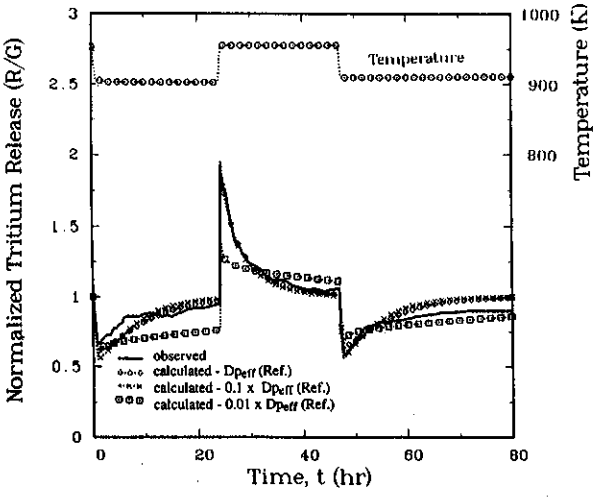

Fig. 2. Effect of the diffusion coefficient in the pore on tritium release profile (LISA1 experiment, runs A-2/A-3/A-4).

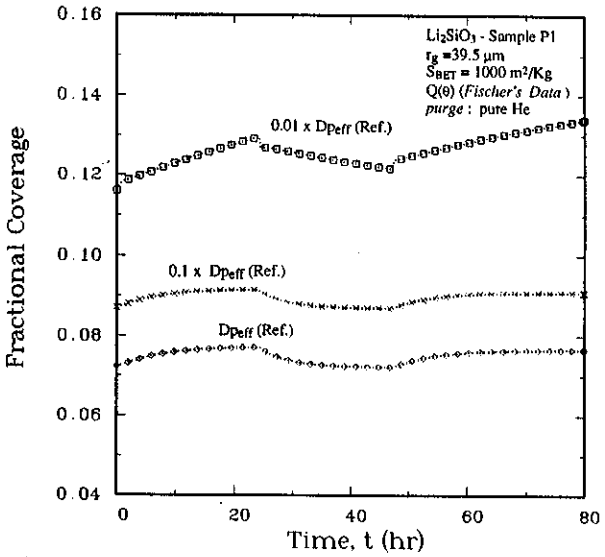

Fig. 3. Effect of the diffusion coefficient in the pore on the tritium coverage at a pore location $z = 0.25z_{ip}$.

part of the experiment time history (cycles A-2, A-3 and A-4 of the LISA1 test matrix including three temperature transients). Three cases were analyzed using for the calculation the data summarized in table 4: (1) $D_{P_{eff}}$(ref.) calculated as we have indicated in the previous section, (2) $0.1D_{P_{eff}}$(ref.) and (3) $0.01D_{P_{eff}}$(ref.). As shown in the figures, the pore diffusion coefficient can strongly affect the release response by controlling the amount of tritium in the pores, and in turn the coverage. There is only a small difference in the tritium release profile for the cases (1) and (2) and they both reproduce quite well the experimentally observed profiles, which tend to give credence to the pore diffusion analysis carried out in the previous section since the value of 0.0033 from eq. (5) corresponds to $0.15D_{P_{eff}}$(ref.). However, the effect on the tritium release is quite marked for the lowest value of the diffusion coefficient which results in a lower peak and a much longer time to return to steady-state due to the slower diffusion of tritium in the pore.

An overall analysis for cycles A-1 through A-5 for the lithium metasilicate sample P1 has also been carried out using $D_{P_{eff}}$(ref.) and the data summarized in table 4. Note that no data were available for the specific surface area of the sample, S_{BET}, and a value of $S_{BET} = 1000$ m^2/kg was chosen based on typical surface areas measured for other silicate samples. The tritium release profile predicted by the model matches quite well the experimentally observed profile, as shown in fig. 4. The tritium release can be seen to be strongly influenced by temperature changes. In particular, a marked tritium release peak occurs in correspondence to a temperature increase, while a profound dip occurs for a temperature decrease. Both the peaks and the dips occur quasi-instantaneously with the temperature changes and no significant time-lags have been observed. After a long irradiation time, there is an indication of a partial degradation of the tritium recovery which could have resulted from either phase dissociation of Li_2SiO_3 or grain growth. The reasonable agreement between the predicted results and the observed data supports the contention that for the range of temperature typical of the experiment under investigation, changes in the tritium release behavior depend mostly on changes in surface coverage. Thus, processes affecting the magnitudes and characteristic times of adsorption and desorption in effect control the rate of tritium release.

For the MOZART experiment, the comparison of the model predictions with the experimental data for the transient tritium release in the aluminate sample S1 after a temperature change are presented for two typical cases (run 3.5 and run 3.6) for a 50 °C decrease and increase in temperature, respectively, and for a helium purge containing 0.01% H_2. For both cases, calculations were done for three values of the pore diffusion coefficient: (1) $D_{P_{eff}}$(ref.) corresponding to an f_{DP} of 0.04 as discussed in the previous section, (2) $0.5D_{P_{eff}}$(ref.), and (3) $0.25D_{P_{eff}}$(ref.). Figs. 5 and 6 show the tritium release profiles normalized to the generation rate for the runs 3.5 and 3.6, respectively. Again, the effect of varying the

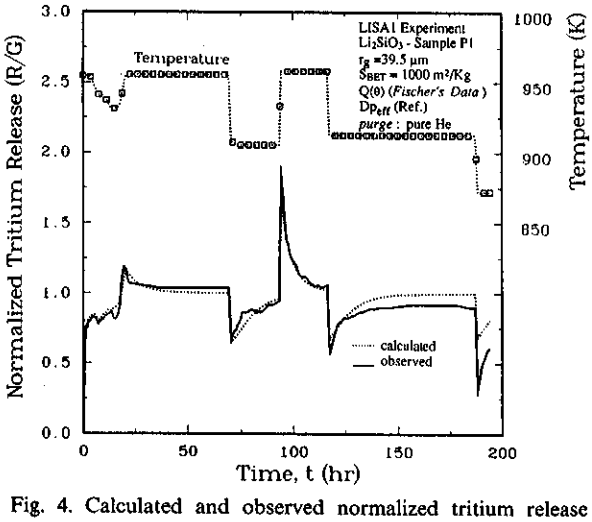

Fig. 4. Calculated and observed normalized tritium release from sample P1 (Li_2SiO_3), LISA1 experiment, runs A-1/A-2/A-3/A-4/A-5.

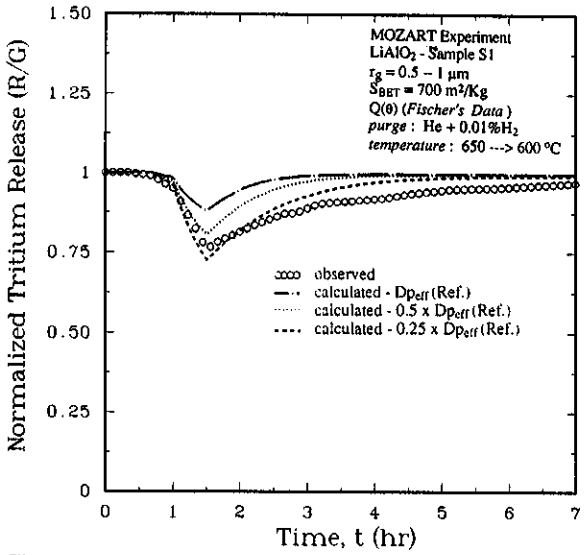

Fig. 5. Calculated release after a temperature decrease at constant purge composition for the aluminate sample S1 (MOZART experiment, run 3.5).

pore diffusion coefficient on the tritium release peak and dip is quite marked and the lowest value of the diffusion coefficient investigated better approximates the experimental results. The trend of the predicted profiles may be explained on the grounds that both the

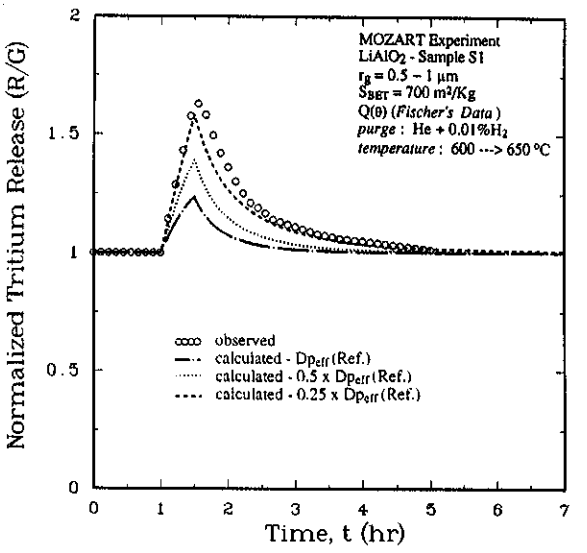

Fig. 6. Calculated release after a temperature increase at constant purge composition for the aluminate sample S1, (MOZART experiment, run 3.6).

magnitude and time scale of tritium release depend strongly on pore diffusion. A very low diffusion coefficient through the pore results in higher tritium partial pressure in the pore and therefore an increase of the tritium coverage. This provides a larger source of tritium and a higher peak tritium release following a temperature rise. Conversely, following a temperature drop transient, more tritium is required to reach quasi-steady-state again and a sharper dip in the tritium release occurs. The time to return to a steady-state normalized tritium release value of 1 is also dependent on the pore diffusion coefficient, more specifically on the time for the tritium-bearing species to diffuse out once they desorb from the surface.

3.2. Transient tritium recovery behavior after a change of purge gas composition

The results of the model presented and discussed so far have shown a reasonably good agreement between the model predictions for the tritium release and the experimental observations for the case of a temperature transient for different constant purge gas compositions and a constant tritium generation rate. However, to fully characterize purge gas effects on the overall tritium release kinetics, the effect of a change of gas composition on the tritium response must be also examined. Several recent in-pile tritium extraction experiments, such as TRIO as indicated by Clemmer et al. [16] and MOZART as reported by Briec [8,9], have shown clearly that the tritium release and, therefore, the inventory evolution are strongly affected by a change in the purge gas composition.

3.2.1. Influence of the adsorption / desorption observed in purge lines

One important issue which needs to be addressed, in particular for the case of a purge gas composition transient, is associated with the potential contribution of adsorption and desorption in the purge lines on the measured tritium release. In each experiment the purge stream, upon leaving the capsule, must traverse a certain length of stainless steel tubing leading to the measurement apparatus. It is clear that certain operating circumstances may enhance the tritium holdup of such lines, or on the other hand increase its release, and the resulting effect of the measured release, downstream of the lines, might not be negligible.

For the case of a temperature change in the sample at constant purge gas composition, the effect of the lines is believed to be relatively small for a constant purge line temperature. In this case, the change of

tritium and hydrogen coverages in the lines, is produced only by relatively small changes in the partial pressure of gas species released from the sample as they flow through the tubes. However, for the case of a purge transient, a change in hydrogen content causes a considerable change in the partial pressure of the hydrogen species flowing through the purge lines and could lead to adsorption or desorption of a large fraction of tritium in the stainless steel tubes. A simple model for the adsorption and desorption in purge lines leading to and away from the solid breeder sample has been developed and used to help in the understanding and interpretation of the discrepancies between observed release results and model predictions for the case of purge transients.

3.2.2. Results of the analysis

The analysis was carried out, using the data summarized in table 4, for the aluminate sample S1 irradiated in the MOZART experiment under three typical transient in purge gas composition at different constant temperature. In run 2.7, the purge gas mixture (He + 0.1% H_2) was replaced by pure helium and the temperature was kept at 650 °C. As a result of the change, a large decrease in tritium concentration in the purge was observed, followed by a slow return to steady-state. According to the indications provided by Briec [17], hydrogen remained in the purge at an impurity level after the purge transient in the experiment. Consequently, the tritium analysis using the model was performed assuming 3 vppm of H_2 in the purge following the transient. However, to investigate the effect of uncertainties in the measurement of the impurity level of the sweeping gas component in the helium purge on the tritium release kinetics, a second case was analyzed with 8 vppm of H_2 in the purge following the transient. The results predicted by the model for the tritium release for the two cases analyzed are shown in fig. 7. The tritium release substantially decreases initially by the change in hydrogen content in the purge. The return to steady-state is slower for the case with the lower final hydrogen impurity level. The analysis shows that, in particular for cases with a "pure" helium purge, even impurity levels of H_2 could affect the release kinetics and should be characterized as part of the experimental and properly accounted for in the modeling.

As before, to investigate the effect of the rate of pore diffusion on the tritium release, three cases were analyzed for the same purge composition change and for a H_2 concentration in the purge after the transient equal to 3 vppm: (1) $D_{p_{eff}}$(ref.), (2) $0.5D_{p_{eff}}$(ref.) and (3) $0.25D_{p_{eff}}$(ref.). The results are shown in fig. 8. Fig. 9

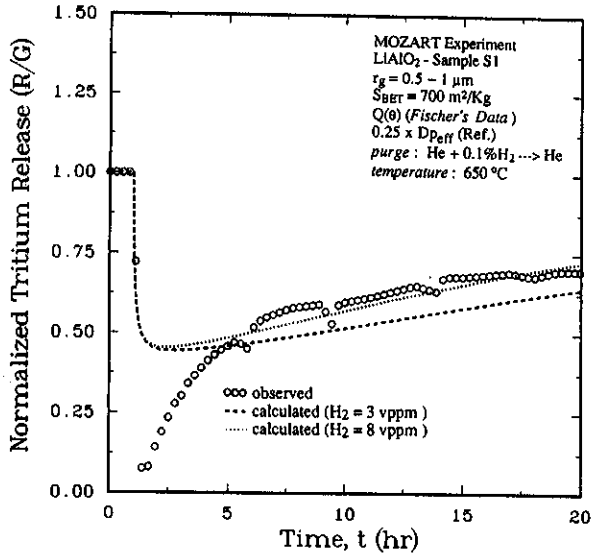

Fig. 7. Effect of very low concentrations of hydrogen on the tritium release profile for a purge transient, (MOZART experiment, run 2.7).

shows the coverages as a function of time for the assumed transient at a pore location of $z = 0.25z_{ip}$ and for the case with $0.25D_{p_{eff}}$. As a result of the change in the hydrogen content in the purge, there is an increase of the tritium coverage and a decrease of the hydrogen

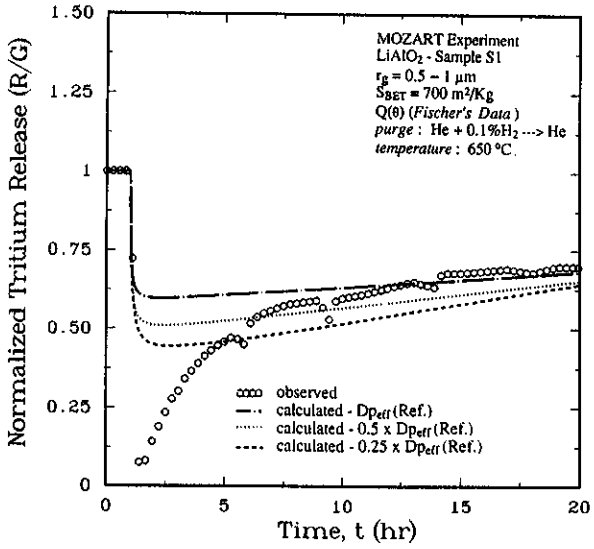

Fig. 8. Effect of the diffusion coefficient in the pore on the tritium release profile for a purge transient, (MOZART experiment, run 2.7).

coverage. There is a reasonable agreement between the model predictions and the measured tritium release, except for the first 2–3 h after the change in purge composition, where the model does not reproduce correctly the observed tritium release dip, and the predictions basically underestimate the tritium retained in the sample. However, in this case, it is likely that a part of the tritium is not retained in the sample but in the lines. To ascertain the influence of the contribution of the line adsorption and desorption on the tritium release and to help in the interpretation of the discrepancies between the observed and predicted profiles, a calculation has been performed using a simple model to evaluate how the tritium and hydrogen coverages on the stainless steel lines between the sample and measuring apparatus change during the purge gas composition transient. The following data and parameters for the purge lines of the MOZART experiment have been assumed for the calculations: line length = 25 m, wall temperature of 25 °C (these lines were not heated), inner tube diameter ≈ 3 mm and heat of adsorption for water on stainless steel ≈ 150 kJ/mol [18].

The corresponding results for tritium and hydrogen coverages are presented in table 5 for different times. The assumed hydrogen concentration is 0.1% initially and is 3 vppm after the transient. The tritium partial pressure is based on a normalized release of 1 initially and on the corresponding experimental values from fig. 8 for times following the transient. The trend of the

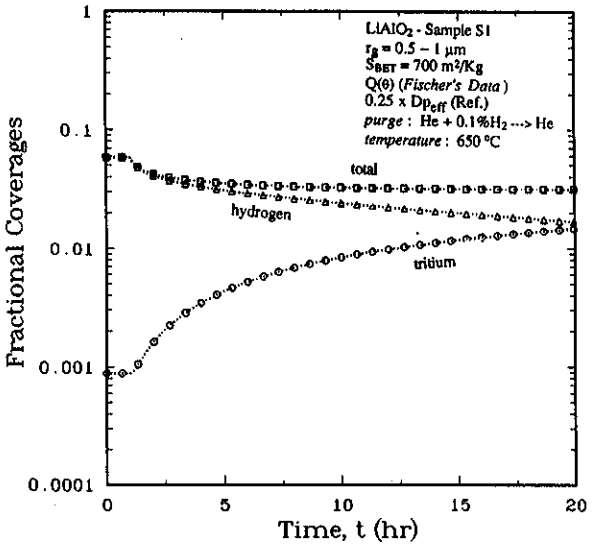

Fig. 9. Effect of a change in purge gas composition on the coverage profiles for 3 vppm H_2 impurity in the purge at a pore location $z = 0.25 z_{ip}$.

Table 5
Values of the hydrogen and tritium coverages on the lines of the tritium release measurement system following a purge gas composition transient (He + 0.1% H_2 ⇒ He) in the $LiAlO_2$ sample S1–run 2.7

Time following transient (h)	Coverages	
	θ_T	θ_H
0	0.002	0.635
2	0.008	0.083
5	0.037	0.069
20	0.050	0.064

evolution of the calculated line coverages seems reasonable and agrees with the indications available from fig. 8, where the shift between the observed and the predicted curve may be interpreted in terms of a tritium holdup on the lines between 2 and 5 h.

On the basis of the coverage values obtained above, a rough estimate of the amount of tritium which is actually retained on the lines has been carried out, considering the change in the tritium coverage and the assumed geometrical quantities and parameters for the lines indicated above. The calculations over the first 5 h following the transient showed that roughly about 4×10^{-7} g of tritium are collected on the lines. This result is of the same order as the difference between the amount of tritium predicted and observed over the first 5 h following the transient, which is about 1.2×10^{-7} g (calculated from the area enclosed within the shift between the observed and predicted profiles for the case with $0.25 D_{P_{eff}}$(ref.) in fig. 8). This result is important and supports the contention presented above that the discrepancies between the observed release and the model predictions for the case of a purge gas composition transient may be due to line effects and, therefore, the interpretation of the result has to be made carefully.

In the experimental run 3.4, the purge composition was changed from pure helium to He + 0.01% H_2. The temperature was unchanged and kept at 650 °C. An impurity level of 3 vppm of hydrogen in the purge was assumed initially for the analysis. Results of the calculation for three values of the pore diffusion coefficient (1) $D_{P_{eff}}$(ref.), (2) $0.5 D_{P_{eff}}$(ref.) and (3) $0.25 D_{P_{eff}}$(ref.) are shown in fig. 10. As a result of the change in hydrogen content, there was a sharp peak in the tritium concentration in the purge stream, followed by a slow return to steady-state. The normalized tritium release R/G (R = tritium release, G = tritium generation) reaches a value of 5.2 in about an hour, then falls to about 1.5 in approximately another two hours, but then

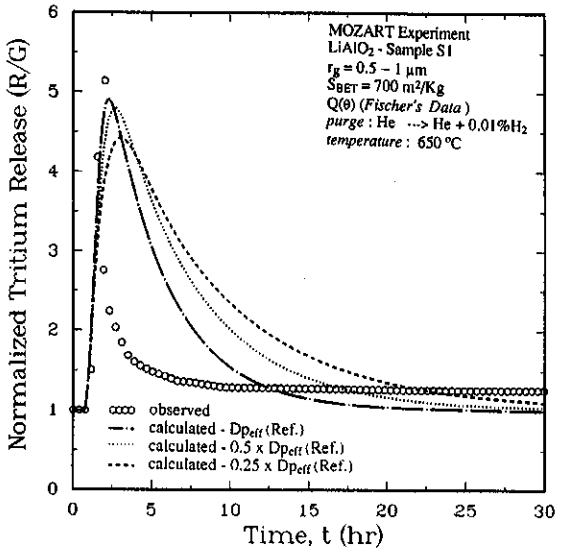

Fig. 10. Effect of the diffusion coefficient in the pore on the tritium release profile for a purge transient, (MOZART experiment, run 3.4).

decreases very slowly to reach a value of about 1.2 after 30 h. It seems reasonable to expect that the steady-state condition ($R/G = 1$) would be reached only after much a longer time. For the case with a $0.25D_{P_{eff}}$(ref.) the peak of the release is ≈ 4.5 and occurs after a time-lag of about 2 h, while for the case with a $0.5D_{P_{eff}}$(ref.) the peak of the release is slightly higher and occurs after a time-lag of about 1 h. In this case, the choice of $D_{P_{eff}}$(ref.) seems to give a better fit to the observed release. However, it is likely that the tritium release behavior is again influenced by adsorption/desorption in the lines. Analogously to the previous case, to roughly estimate this influence, an evaluation of the tritium and hydrogen coverages on the lines was carried out assuming the same reference data as before.

The results for tritium and hydrogen coverages are presented in table 6 for different times. Based on this, the amount of tritium released from the lines is estimated to be about 1×10^{-6} g. For the case of $0.25D_{P_{eff}}$(ref.), assuming the observed normalized tritium release remains at 1.2 over a long time, the difference between the observed and predicted amount of tritium release reaches 1×10^{-6} g after about 60 h. Fig. 11 shows for $0.25D_{P_{eff}}$(ref.) the behavior of the coverages at a location of $z = 0.25z_{ip}$ along the interconnected pore system, and indicate clearly the decrease in the tritium adsorbed on the surface as it is replaced by hydrogen (swamping effect). In other words, adding

Table 6
Values of the hydrogen and tritium coverages on the lines of the tritium release measurement system following a purge gas composition transient (He ⇒ He + 0.01% H_2) in the $LiAlO_2$ sample S1–run 3.4

Time following transient (h)	Coverages	
	θ_T	θ_H
0	0.076	≈ 0
2	0.049	0.324
5	0.017	0.345
30	0.013	0.348

hydrogen (protium) to the purge results in a build-up of hydrogen partial pressure in the network of pores, and in an increase of the adsorption flux of hydrogen-bearing species on the surface. As a result of the competition for active sites at the surface, hydrogen (which is generally present in much larger quantity than tritium) basically replaces the tritium collected on the surfaces, whose coverage decreases.

Finally, for the experimental run 4.4, the purge gas composition was changed from He + 0.01% H_2 to He + 0.1% H_2 and the temperature of the sample was unchanged and kept equal to 550 °C. Simultaneously with the change in purge gas composition an unexpected $\approx 16\%$ decrease of the neutron flux occurred in the reactor between 1 and 2 h. The modeling analysis was carried out including both the purge and neutron flux

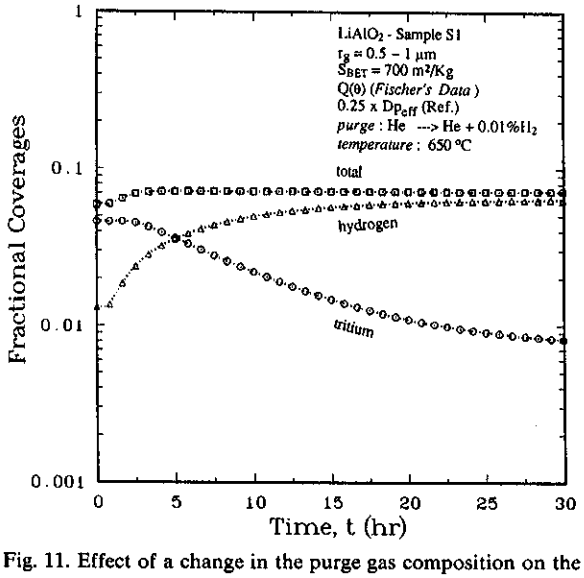

Fig. 11. Effect of a change in the purge gas composition on the coverage profiles at a pore location $z = 0.25z_{ip}$.

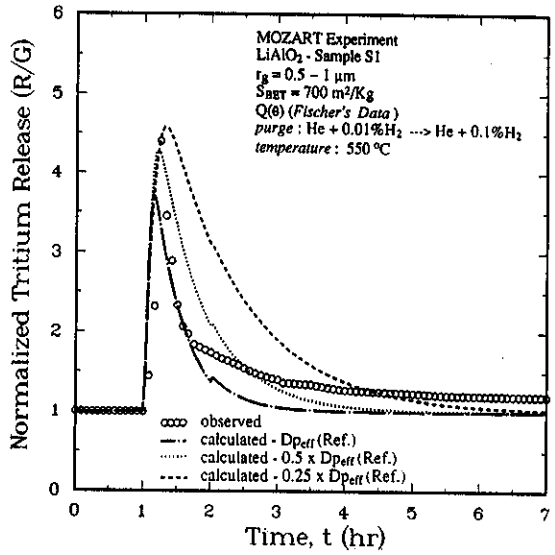

Fig. 12. Effect of the diffusion coefficient in the pore on the tritium release profile for a purge transient, (MOZART experiment, run 4.4).

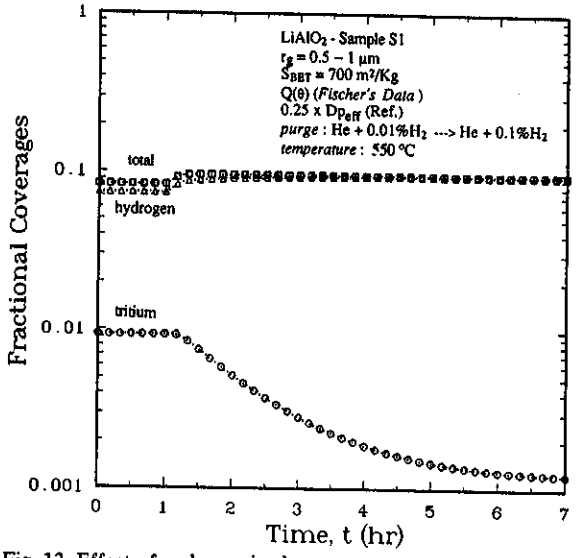

Fig. 13. Effect of a change in the purge gas composition on the coverage profiles at a pore location $z = 0.25z_{ip}$.

(i.e., tritium generation rate) transient histories. The corresponding result for the release as a function of time is shown in fig. 12. Again, the analysis was carried out for D_{Peff}(ref.), $0.5D_{Peff}$(ref.), and $0.25D_{Peff}$(ref.). As a result of the change in purge gas composition, a sharp peak occurred quasi-instantaneously followed by a slow decrease to the steady-state value which had not yet been reached after 7 h.

A reasonably good agreement exists between the model predictions and the observed experimental results, with the best fit corresponding to about $0.5D_{Peff}$(ref.). For this case also, a rough estimate of the tritium which may have been released from the lines has been made using the same approach described before. The results for the tritium and hydrogen coverages on the stainless steel tubes at typical times of the transient are summarized in table 7. The analysis indicates that the increase in hydrogen concentration in the purge causes a decrease of the amount of tritium collected on the lines which is basically replaced by the hydrogen and is released. The estimation of the amount of tritium released from the lines has been done by considering the change in tritium coverage and assuming the same reference data as before. Based on this, for a change in tritium coverage from 0.011 to 0.003, about 1×10^{-7} g of tritium would be released from the lines. For the case of $0.25D_{Peff(ref)}$ the difference between the observed and predicted amount of tritium reaches 1×10^{-7} g after approximately 15 h. For this case, fig. 13 shows the evolution of the coverages at a pore location $z = 0.25z_{ip}$.

Table 7
Values of the hydrogen and tritium coverages on the lines of the tritium release measurement system following purge gas composition transient (He+0.01% H_2 ⇒ He+0.1% H_2) in the $LiAlO_2$ sample S1–run 4.

Time following transient (h)	Coverages	
	θ_T	θ_H
0	0.011	0.349
2.5	0.008	0.629
5.5	0.003	0.634
7	0.002	0.634

4. Summary

Tritium transport and release from fine-grained lithium-base ceramic breeders for fusion applications is characterized by a complex sequence of processes which cannot be predicted accurately using a simple model. Effective bulk diffusion with and without a desorption flux boundary condition has been the basis of past models describing tritium release from solid breeders. This has led to difficulties and confusion in the interpretation of experimental data and in the understanding of the effect of individual material properties and operating conditions on the tritium release behavior.

The tritium transport model MISTRAL has been recently developed for the interpretation of results available from in-pile tritium release experiments in lithium-base ceramics, as well as for providing a design tool to forecast the behavior of solid breeder blankets under typical fusion operation conditions. The model includes several individual transport mechanisms such as grain diffusion, grain boundary diffusion, adsorption and desorption at the solid/gas interface and diffusion through the network of interconnected pores and has both multiregion and multispecies capabilities. A rate theory formulation has been used to include the different fluxes which link the surface adsorption/desorption model to the diffusive models in the solid and in the gas phases.

The model has been used to analyze some of the most recent results available from in-pile tritium release experiments such as LISA1 and MOZART. With the aim to perform a plausible analysis, the experimental conditions for each sample were reproduced as closely as possible, and most importantly, measured physical and chemical properties of the breeder materials investigated were used, when available, without any attempt to adjust them in order to reproduce the observed results.

The cases analyzed were: (1) release from a metasilicate sample under temperature transient with a constant pure helium purge gas composition; (2) release from an aluminate sample under temperature transients with a constant protium-containing helium purge gas composition; (3) release from the same aluminate sample at constant temperature under a purge gas composition change for a helium purge containing protium as a tritium sweeping component. The model predictions showed reasonably good agreement with the experimental observations, in particular for temperature transients, and they were obtained using a detailed set of material properties and minimizing the number of parameters (i.e., controlling knobs) that can be varied to match the model to the experimental results.

Based on the calibration analysis carried out for different ranges of operating conditions, the following observations can be made:

- For the cases analyzed, the model results illustrate the importance of the adsorption and desorption processes in conjunction with local pore concentrations. In this regard, the solid breeder microstructure is a determinantal factor which needs to be properly characterized before and after irradiation, since microstructure characteristics could change through sintering and grain growth for example. In particular, the specific surface area is a key parameter for adsorption/desorption calculations, while the magnitude and distribution of pore sizes and the amount of open interconnected porosity are important parameters in determining the effective pore diffusion coefficient and the tortuosity factor, respectively. These results tend to contrast with the indications provided by some of the simple tritium transport models developed in the past and represents a major shift in the interpretation of the predictions. Indeed, all the existing models tend to oversimplify the diffusion step through the network of interconnected pores and neglect any kind of linking between the surface and the pore regions. This coupling is crucial to correctly account for the fact that the breeder surface acts like a key interface controlling the filling of surface adsorption sites by tritium atoms from the bulk and from the pore, as well as the rate of desorption to the pore.
- In theoretical models of tritium release from ceramic breeders, the activation energy for desorption, and particularly its dependence on the degree of coverage for adsorption of gases like H_2 and $H_2O_{(g)}$, are important variables which influence the amount of gas holdup on the breeder surfaces and the underlying release kinetics.
- Tritium and hydrogen adsorption to and desorption from the inner surface of purge lines can substantially affect the tritium release, in particular in the case of purge hydrogen content transient, and make the interpretation of the results available from in-pile tritium release experiments particularly difficult.

On the basis of the indications presented above and with the aim to improve the predictive capabilities of the model and to help in gaining understanding of the discrepancies between solid breeder tritium release results and model predictions, specific recommendations are proposed for planning new irradiation experiments and laboratory studies in order to maximize their benefits.

Irradiation experiments: greater attention has to be given to pre- and post-test characterization of the materials used in irradiation experiments, in particular for better characterization of the specific surface area, the fraction of open porosity and the magnitude and distribution of pore sizes, which have been found to be major parameters affecting the tritium release. Irradiation experiments should include long sample exposure to better observe effects of burnup/irradiation damage upon tritium release and/or tritium retention.

Laboratory studies: because of the importance of surface processes and of the scarcity of property data, it is particularly important that the activation energies for

adsorption on and desorption from the major candidate ceramics be determined through laboratory studies for both H_2 and H_2O as a function of the surface coverage and of the temperature. Experimental information should be obtained on bonding states between protium and the ceramic. Interfacial/surface properties on the ceramic-H_2O/H_2 system should emphasize the differences in ceramic stoichiometry in the surface region versus that of the bulk region. Although not included in the model for the present study, the formation of $LiOT_{(s)}$ within the breeder matrix can be important at low temperatures while the solubility of $LiOT_{(g)}$ in the breeder may become substantial at high temperatures and partial pressures, particularly in lithium oxide for which some data exist. In this concern, LiOT formation and dissociation in all major candidate ceramics as a function of partial pressure and temperature should be determined. Modelers will be greatly helped when these results become available.

Nomenclature

D_g intragranular tritium diffusion coefficient (m^2/s);
D_{g0} pre-exponential factor for intragranular diffusion (m^2/s);
D_p pore diffusion coefficient based on average pore radius ($m^2/2$);
$D_{p_{ave}}$ average pore diffusion coefficient (m^2/s);
$D^{(i)}_{p_{eff}}$ effective diffusion coefficient in the pore for species (i) (m^2/s);
E_{ads} activation energy for dissociative adsorption (J/mol);
E_β activation energy for adsorption of atoms from the bulk (J/mol);
E_{des} activation energy for associative desorption (J/mol);
E_g activation energy for grain diffusion (J/mol);
f_{DP} ratio of $D_{p_{eff}}$ to D_p;
$\mathscr{G}$ tritium production rate per unit volume (atoms/m^3 s);
L_e effective length for the interconnected pore system (m);
l_{p_j} length of cylindrical pore j (m);
L_p ratio of lengths of two cylindrical pores in series;
N_S density of sites (in general $\approx 1 \times 10^{19}$ sites/m^2);
$Q(\theta)$ heat of adsorption as a function of coverage (J/mol);
$\mathscr{R}$ tritium release rate (atoms/grain s);
r_{ip} average radius of interconnected pore system (m);
r_g average grain radius (m);
r_{p_j} radius of pore j (m);
R_p ratio of radii of two cylindrical pores in series;
S_{BET} specific surface area of the breeder (m^2/kg);
T absolute temperature (K);
z_{ip} equivalent interconnected pore system length ($z_{ip} = L_e$) (m).

Greek Letters

β_0 pre-exponential factor for adsorption from the bulk (m/s);
ϵ_p porosity of the breeder;
ϵ_{p_j} open porosity associated with specific mean pore size j;
Γ purge flow rate (l/h);
ϕ sample diameter (m);
θ total coverage (fraction of adsorption sites occupied);
θ_H hydrogen coverage;
θ_T tritium coverage;
θ_0 fraction of the surface uncovered by any atom;
ρ solid theoretical density (kg/m^3).

Glossary

ANL	Argonne National Laboratory
BEATRIX	Breeder Exchange Matrix
BET	Brunauer–Emmett–Teller
CEA	Commissariat a l'Energie Atomique
JAERI	Japan Atomic Energy Research Institute
JRR	Japanese Research Reactor
MISTRAL	Model for Investigative Studies of Tritium Release in Lithium Ceramics
MOZART	Melusine Oxide Zirconate Aluminate Release of Tritium

Acknowledgements

Most of the research reported here has been carried out as part of a doctoral thesis dissertation by the first author. We would like to thank Dr. M. Briec, Dr. B. Rasneur and Dr. N. Roux for providing us with very detailed information on the MOZART experiment, Dr. Z. Gorbis for his contribution on the pore diffusion analysis, and Dr. M. Billone for his valuable input. This work was supported by the US Department of Energy under grant #DE-FG03-86ER52123.

References

[1] J.P. Kopasz and C.E. Johnson, Progress Report on Fusion Reactor Materials, DOE/ER-0313/4 (March 1988).

[2] A.R. Raffray, G. Federici and M.A. Abdou, in: Proc. 2nd Specialists' Workshop on Modeling Tritium Behavior in Fusion Blanket Ceramics, Indianapolis, 1989, p. 81.

[3] G. Federici, A.R. Raffray and M.A. Abdou, in: Proc. 2nd Int. Symp. on Fabrication and Properties of Lithium Ceramics, Indianapolis, 1989.

[4] G. Federici, Ph.D. Dissertation, University of California at Los Angeles (October 1989).

[5] G. Federici, A.R. Raffray and M.A. Abdou, companion paper, J. Nucl. Mater. 173 (1990) 185.

[6] H. Werle, J.J. Abassin, M. Briec, R.G. Clemmer, H. Elbel, H.E. Hafner, M. Masson, P. Sciers and H. Wedemayer, in: Proc. 2nd Int. Conf. on Fusion Reactor Materials (ICFRM-2), Chicago, 1986, J. Nucl. Mater. 141–143 (1986) 321.

[7] M. Briec, J.J. Abassin, C.E. Johnson, M. Masson, N. Roux, and H. Watanabe in: Proc. 15th Symp. on Fusion Technology, Utrecht, September 1988.

[8] M. Briec in: Proc. 2nd Int. Symp. on Fabrication and Properties of Lithium Ceramics, Indianapolis, 1989.

[9] M. Briec et al., in: Proc. 2nd Specialists' Workshop on Modeling Tritium Behavior in Fusion Blanket Ceramics, Indianapolis, 1989, p. 1.

[10] A.K. Fischer and C.E. Johnson, in: Proc. 8th Topical Meeting, Salt lake City, Utah, 1988, Fusion Technol. 15 (1988) 1212.

[11] H.L. Gruber, J. Phys. Chem. 66 (1962) 48.

[12] N. Wakao and J.M. Smith, Chem. Eng. Sci. 17 (1962) 825.

[13] J.H. Krasuk and J.M. Smith, AIChE J. 18 (1972) 506.

[14] H. Elbel, in: Proc. 3rd Int. Conf. on Fusion Reactor Materials (ICFRM-3), Karlsruhe, Fed. Rep. Germany, October 1988, J. Nucl. Mater. 155–157 (1988) 480.

[15] A.S. Michaels, AIChE J. 270–271 (June 1959).

[16] R.G. Clemmer et al., The TRIO Experiment Report, ANL-84-55, Argonne National Laboratory (September 1984).

[17] M. Briec, The MOZART Experiment Report, Commissariat à l'Energie Atomique – IRDI-DESIGCP CEN – Grenoble, France, July 1989.

[18] B.M.W. Trapnell and D.O. Hayward, Chemisorption, 2nd Ed. (Butterworths, London, 1964).

[19] K. Okuno and H. Kudo, in: Proc. 1st Int. Symp. on Fusion Nuclear Technology, Tokyo, 1988, Fusion Eng. Des. 8 (1989) 355.

[20] M.A. Pick and K. Sonnenberg, J. Nucl. Mater. 131 (1985) 208.